Asociación Argentina
de Mecánica Computacional

Mecánica Computacional Vol XXIX, págs. 5-19 (artículo completo)
Eduardo Dvorkin, Marcela Goldschmit, Mario Storti (Eds.)
Buenos Aires, Argentina, 15-18 Noviembre 2010

CONTINUUM AND DISCRETE APPROACHES FOR FAILURE ANALYSIS OF FIBER-REINFORCED CONCRETE

G. Etse[a], A. Caggiano[b] and S. Vrech[c]

[a]*CONICET, University of Buenos Aires, Argentina.*

[b]*Department of Civil Engineering, University of Salerno, Salerno, Italy*

[c]*CONICET, National University at Tucuman, Argentina*

Keywords: FRC, strain-hardening/softening behaviors, continuum-based microplane theory, mesoscopic modeling.

Abstract. As extensively accepted, fiber inclusions lead to significant improvements of post-cracking behavior of mortar composites by bridging cracks and providing resistance to crack opening processes. Typically localized failure modes of plain concrete or other mortar composites may turn quasi-ductile through the addition of steel fibers in cement mortar. In this case, the development of multiple crack patterns lead to strain-hardening/softening processes characterized by relatively large energy absorption prior to fracture localization. From the structural standpoint, fiber reinforced concrete structures (FRCS) exhibit superior ductility not only when subjected to compressive but also to tensile loading.

In this work fiber reinforced concrete is analyzed and modeled with two different approaches. On the one hand, a macroscopic continuum (smeared-crack) evaluation based on non-linear microplane theory is presented. Following approaches recently proposed in Pietruszczak and Winnicki (2003) and others, the microplane model is formulated on the basis of the mixture theory, by Truesdell and Toupin (1960), to describe the coupled action between concrete and fiber reinforcements. On the other hand, a constitutive theory is presented to model the non-linear response of fiber reinforced mortar-mortar interfaces in the framework of discrete approach for failure analysis. Final aim of this strategy is the mesoscopic observation of FRC failure behavior based on FE discretizations accounting for the three main concrete constituents: aggregates, mortar and mortar-aggregate interfaces. Non linear behavior of fiber reinforced mortar is modeled by inelastic mortar-mortar interfaces where fibers are considered to be located. The interface model considers the quadratic hyperbola in terms of contact stresses proposed by Carol et al. (1997) as mortar/concrete maximum strength criterion. While the microplane model is founded on a linear function for shear and normal strengths. Their softening laws for post-peak behavior are formulated in terms of the fracture energies release under mode I, II and/or mixed failure modes. Similarly to the macroscopic smeared-crack based model, the mixture theory is taken into account to model the composites mortar-mortar interfaces reinforced with steel fibers. Also the fiber-concrete and fiber-mortar interactions in the form of fiber debonding and dowel effects are similarly treated in both macroscopic and interface models.

After describing both constitutive models the paper focuses on numerical analysis of FRC failure behavior. The main objective of these analyses is to evaluate the capabilities of the proposed models and numerical tools to capture the transition from brittle to ductile behavior of fiber-reinforced concrete when different levels of fiber contents are considered as well as different fiber directions.

1 INTRODUCTION

Cement-based composites, like concrete or mortar, represent structural materials commonly used in civil engineering. They are prevalently utilized for members in predominantly compressive stress state being characterized by excellent mechanical properties in compression. Weaker performances are expected under more general load conditions, especially under tensile or shear stresses, that requires a steel reinforcement to improve the material resistance. The poor mechanical properties of plain concrete under those stress states can be mitigated by adding short steel fibers into the cementitious matrix.

Furthermore, high-performance fiber-reinforced concrete (HPFRC) that exhibit strain hardening behavior and multiple cracking response under tensile loading can be obtained adding short steel reinforcements (Naaman and Reinhardt, 2006). Actually, HPFRC may achieve ductility, durability and high energy absorption capacity compared with plain concrete or conventional fiber-reinforced concrete (FRC), this latter characterized by low fiber content into the past.

Several models, analytical approaches and numerical formulations have been developed to represent the mechanical behavior of fiber reinforced concrete (FRC). Among them, several models based on the plasticity theory are presented into the scientific literature (Hu et al., 2003; Seow and Swaddiwudhipong, 2005); other authors treats the FRC material in the frame of the continuum damage mechanism theory (CDM) (Li and Li, 2001). A rather innovative approach has been inspired to the so-called microplane model (Beghini et al., 2007; Vrech et al., 2010). Moreover, an analytical model to evaluate the prevailing bond characteristics of the composite is proposed by Banholzer et al. (2006).

In the last decades meso-mechanical approaches have been utilized for discretizing the first level of materials (meso-structure), by assigning to each material component its individual geometrical and mechanical properties. The so-called meso-structure can be used in several varieties such as lattice models (Lilliu and van Mier, 2003), particle models (Zubelewicz and Bazant, 1987), a combination of the particle and lattice model (Cusatis et al., 2010) and continuum meso-models (Carpinteri et al., 2010; Lopez et al., 2008a,b; Lorefice et al., 2008; Caggiano et al., 2010). These approaches provide a much more powerful and physically-based description of the material behavior, modeling with special accuracy the fracture processes and the mechanical properties of plain and fiber reinforced concretes. The apparent macroscopic behavior observed is a direct consequence of the more complex mesoscopic phenomena that take place at the level of the material heterogeneities. The principal disadvantages of these approaches are related, on the one hand, to the higher computational cost, and on the other hand, to the elevate number of variables involved in the model formulation.

The present work deals with the failure analysis of FRC material by means both macro and mesoscopic levels of observation. In both approaches the mixture theory is used as basis for simulating the interaction between cementitious matrix and steel fibers. The main objective of this work is to evaluate the fundamental properties of the FRC during monotonic loading beyond the elastic range.

For the 2D mesoscopic analysis, the FRC has been considered as a three phase material composed by: (i) aggregate, (ii) mortar and (iii) the interfaces between them. The non-linear behavior of steel fiber reinforced mortar is fully captured by means the zero-thickness joint elements as schematized in Fig. 1. For this purpose the original zero-thickness interface model outlined in Carol et al. (1997) has been reformulated to include the interaction between steel fibers and mortar based by means the mixture theory also used in Oliver et al. (2008).

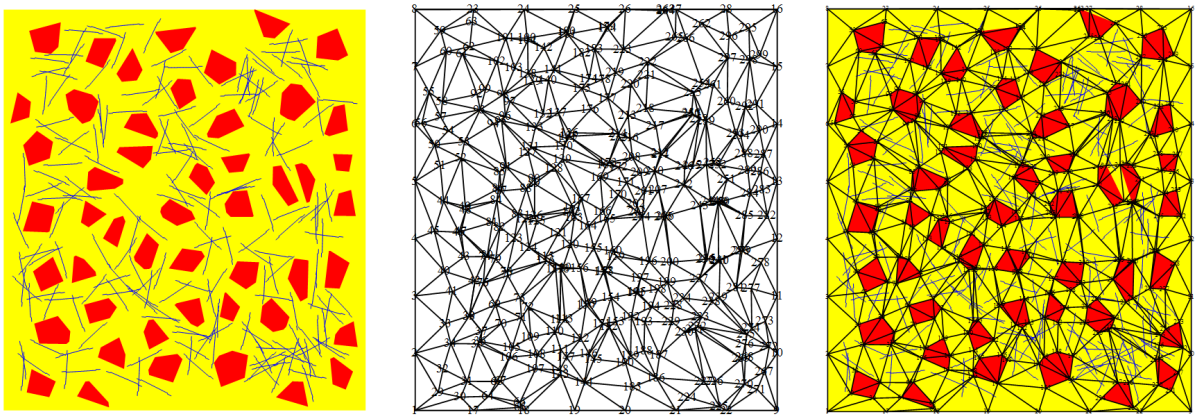

Figure 1: 2D meso-structure configuration.

On the other side the macroscopic approach is based on the microplane theory combined with the flow theory of plasticity in which the maximum strength criterion is given with a linear function of shear and normal microplane strengths. As for the discontinuity approach the composite mixture theory is utilized to account the interaction between steel fibers and concrete, considering now the material as a macroscopic continuum medium.

The numerical analysis presented in this work include predictions of both approaches about FRC failure analyses. The results demonstrate the potentials of the mesoscopic approach to evaluate relevant aspects captured by means the proposed model, i.e. the direction of the fibers, the diameter and length utilized, the amount of the fibers and so on. On the other hand, good results can be obtained by means the microplane based theory allowing the consideration of arbitrary and multiple directions for steel fibers and, eventually, of non-homogeneous materials.

2 COMPOSITE MATERIAL MODELLING

As in the classical plasticity theory the proposed two models have been formulated in incremental form in which the stress-strain relationship of the composite model can be expressed in a unified compact form as

$$\dot{\boldsymbol{\sigma}} = \boldsymbol{E}^{ep} \cdot \dot{\boldsymbol{\epsilon}}. \tag{1}$$

being $\dot{\boldsymbol{\sigma}}$ y $\dot{\boldsymbol{\epsilon}}$ the stress and strain tensors rate, respectively.

According to the basis of the mixture theory, the composite is considered as a continuum in which each infinitesimal volume is ideally occupied by all the components. Each component is subjected to the same strain field while the corresponding composite stresses are given by the weighted sum of the stresses on each component. For the same assumption follows that the constitutive tangent operator $\boldsymbol{E}^{ep}$, is given by the following expression

$$\boldsymbol{E}^{ep} = \rho^m \boldsymbol{C}^{ep} + \xi^f \rho^f E_f^{ep} \boldsymbol{B}_f^{ep}\left(\boldsymbol{n_f}, \boldsymbol{n}_f^t\right) + \xi^f \rho^f G_f^{ep} \boldsymbol{D}_f^{ep}\left(\boldsymbol{n}_{f,T}, \boldsymbol{n}_{f,T}^t\right) \tag{2}$$

depending on the volumetric fraction $\rho^{\#}$ of each component; $\boldsymbol{n}_f$ and $\boldsymbol{n}_{f,T}$ are two unit vectors identifying the parallel and the orthogonal direction of a generic fiber respect to the global Cartesian reference system. The superscripts m and f refer to "concrete matrix" and "fibers", respectively, while the superscript t represents the transposition operation for tensors; $\xi =$

$1-a\rho^f$ (with a model parameter) is a reductive coefficient that considers the minor effectiveness of a single fiber as the reinforcement contents increase. $\boldsymbol{B}_f^{ep}$ and $\boldsymbol{D}_f^{ep}$ are tensorial operators constructed with the direction normal and tangential of the single fiber.

In Eq. (2) the following tangent operators have been utilized

$$\begin{aligned} \boldsymbol{C}^{ep} &= \partial\boldsymbol{\sigma_m}/\partial\boldsymbol{\epsilon_m}; \\ E_f^{ep} &= d\sigma_f/d\varepsilon_N; \\ G_f^{ep} &= d\tau_f/d\varepsilon_T. \end{aligned} \tag{3}$$

General aspects of constitutive formulation, which models the mechanical behavior of both continuum and interface mediums in presence of steel fibers, are given as follows:

- *fracture-based plain material models*: each constitutive model is formulated in terms of normal and shear stresses ($\boldsymbol{\sigma_m}$) corresponding to the relative strains ($\boldsymbol{\epsilon_m}$), also known as "interface stresses" (and "interface relative displacements") for the joint model and "microscopic stresses" (and "microscopic strains") for the microplane analysis. Further details of each specified model have been given in the Sections 3 and 4.

- *fiber bond-slip (Section 5.1)*: a global constitutive model ($\sigma_f - \varepsilon_N$ law) for the debonding fiber process is considered as a combination of two serial response such as the uniaxial fiber behavior and the dissipative bond-slip between fiber-to-concrete interface.

- *dowel action* of short reinforcements (outlined in Section 5.2) in concrete is also modeled in a smeared form considering the fiber as a beam on elastic foundation. The dowel action-displacement response is expressed in terms of dowel stress vs strain ($\tau_f - \varepsilon_T$) in order to be compatible with general formulation given in Eq. (2).

Both the bond-slip model as well as the dowel fiber-to-concrete behavior are similarly considered in both meso- and macro-scopic approaches.

3 ZERO-THICKNESS JOINT LAW

Following approaches recently used in literature, e.g. Lopez et al. (2008a,b); Lorefice et al. (2008), the overall analysis are based on the assumption that continuum mortar and coarse aggregate elements are assumed as linear elastic then the non-linear dissipative behavior is fully considered along the interfaces.

The incremental stress-displacement relationship is given by the following expression

$$\dot{\boldsymbol{t}} = \boldsymbol{E}^{ep} \cdot \dot{\boldsymbol{u}} \tag{4}$$

where $\boldsymbol{t}^t = [\sigma, \tau]$ and $\boldsymbol{u}^t = [u, v]$ are two vectors, called σ_m and ϵ_m in the general Eq. (3) that represent the relative normal/tangential stresses and displacements, respectively. The constitutive tangent second-order tensor $\boldsymbol{E}^{ep}$, based on the general expression given in Eq. (2), can be specified now as

$$\boldsymbol{E}^{ep} = \rho^m \boldsymbol{C}^{ep} + \xi^f \rho^f E_f^{ep} \boldsymbol{n}_f \boldsymbol{n}_f^t + \xi^f \rho^f G_f^{ep} \boldsymbol{n}_{f,T} \boldsymbol{n}_{f,T}^t \tag{5}$$

in which $\boldsymbol{C}^{ep} = \partial\boldsymbol{t}/\partial\boldsymbol{u}$ is a second-order tangent operator referred to plain interface, while E_f^{ep} and G_f^{ep} have been defined in Eq. (3).

The elasto-plastic formulation of the plain interface model can be defined in incremental form as follows

$$\dot{\boldsymbol{t}} = \boldsymbol{C} \cdot (\dot{\boldsymbol{u}} - \dot{\boldsymbol{u}}^{cr}) \tag{6}$$

where $\dot{\boldsymbol{u}}^{cr}$ is the incremental crack opening components and $\boldsymbol{C}$ defines a fully uncoupled elastic contact

$$\boldsymbol{C} = \begin{pmatrix} k_N & 0 \\ 0 & k_T \end{pmatrix}. \tag{7}$$

The model is based on the original loading criterion (Carol et al., 1997) of the interface constitutive model defined as

$$f = \tau^2 - (c - \sigma \tan\phi)^2 + (c - \chi \tan\phi)^2 \tag{8}$$

where the tensile strength χ (vertex of hyperbola of Fig. 2), the shear strength c (cohesion strength) and the internal friction angle ϕ are model parameters. The evolution of fracture process is driven by the cracking parameters χ, c and $\tan\phi$, which depends on the energy release during the interface degradation W_{cr} respect to the energy capacity absorption of the contact in mode I and II, G_f^I and $G_f^I I$ respectively. Further details are given in Carol et al. (1997).

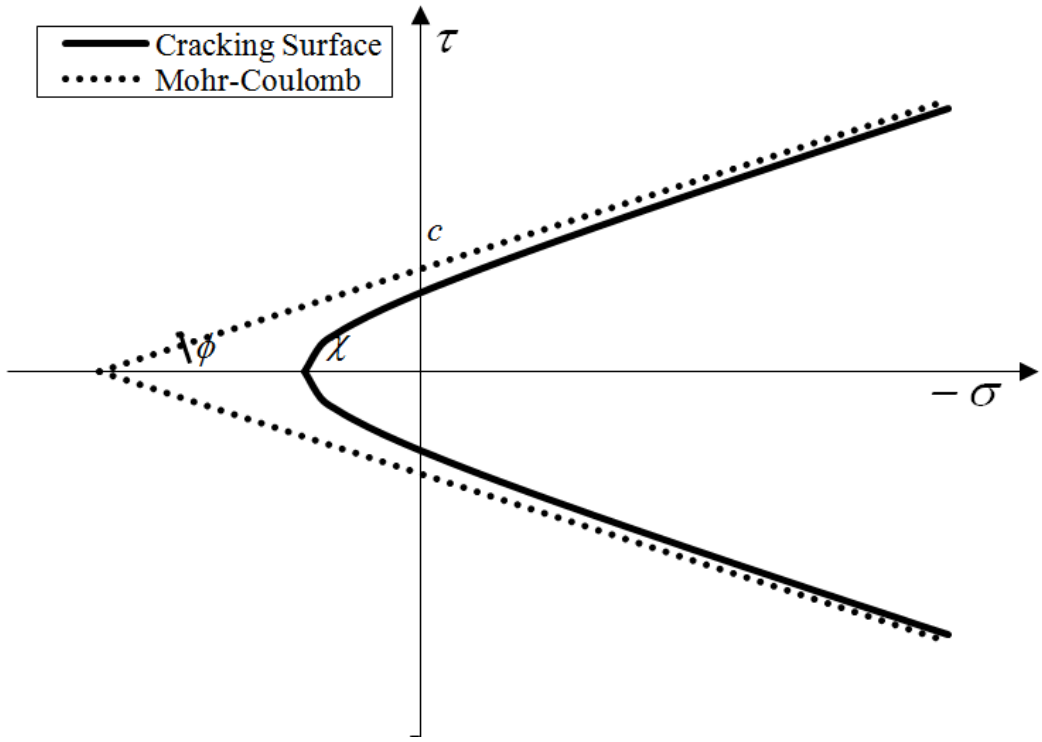

Figure 2: Three-parameter loading criterion.

4 MACROSCOPIC MODEL BASED ON MICROPLANE THEORY

Instead of the existing spherical microplanes models, see a.o. Beghini et al. (2007); Carol et al. (2001); Kuhl et al. (2001) the proposed constitutive theory considers 2D stress and strain fields while uses disk microplanes according to the proposal by Park and Kim (2003). As a

result, a less number of microplanes is required. According to this approach, the fiber-reinforced concrete is idealized as a disk of unit radius and constant thickness b which agrees with that of the analyzed material patch, see Fig. 3.

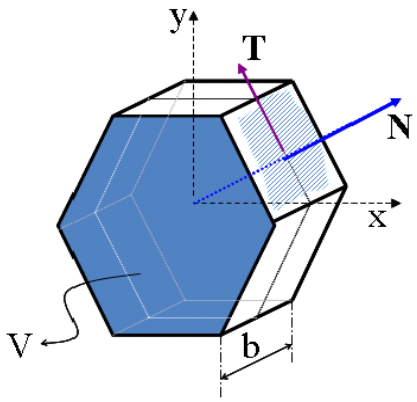

Figure 3: Proposed disk microplanes by Park and Kim (2003).

The following assumptions are considered:

- Macroscopic stresses are uniform in the disk and are equilibrated by the surface tractions on the microplanes.
- Microscopic strains in normal (ε_N) and tangential ($\boldsymbol{\varepsilon}_T$) directions to each microplane with normal direction $\boldsymbol{n}$, are obtained from macroscopic strains $\boldsymbol{\varepsilon}$ (kinematic constrains) as

$$\varepsilon_N = n_i n_j \varepsilon_{ij} \tag{9}$$

$$\varepsilon_{Tr} = \frac{1}{2}\left[n_i \delta_{jr} + n_j \delta_{ir} - 2 n_i n_j n_r\right] \varepsilon_{ij} \tag{10}$$

- Normal and tangential microscopic stresses $\boldsymbol{t} = [\sigma_N, \boldsymbol{\sigma}_T]$ are obtained from the microscopic free energy potential ψ_0^{mic}

$$\sigma_N = \frac{\partial\left[\rho_0 \psi_0^{mic}\right]}{\partial \varepsilon_N} \quad , \quad \boldsymbol{\sigma}_T = \frac{\partial\left[\rho_0 \psi_0^{mic}\right]}{\partial \boldsymbol{\varepsilon}_T} \tag{11}$$

being ρ_0 the material density. The macroscopic free-energy potential per unit mass of material in isothermal conditions, $\psi_0^{mac}(\boldsymbol{\varepsilon}, \boldsymbol{\kappa})$, with $\boldsymbol{\kappa}$ a set of thermodynamically consistent internal variables, results

$$\psi_0^{mac} = \frac{1}{b\pi} \int_V \psi_0^{mic}(\boldsymbol{t}_\varepsilon, \boldsymbol{\kappa})\, dV \tag{12}$$

being V the disk volume.

4.1 Microplane constitutive laws

The microplane constitutive law is based on the mixture theory by Truesdell and Toupin (1960) and, similarly to the interface model formulation used in the analysis at the mesoscopic level of observation, on the hypothesis of the composite model by Oliver et al. (2008).

Then, the constitutive tangent operator $\boldsymbol{E}^{ep}$, given by Eq. (2), adopts the following expression

$$\boldsymbol{E}^{ep} = \rho^m \boldsymbol{C}^{ep} + \rho^f E_f^{ep} (\boldsymbol{n} \otimes \boldsymbol{n}) \otimes (\boldsymbol{n} \otimes \boldsymbol{n}) + 4\rho^f G_f^{ep} (\boldsymbol{n} \otimes \boldsymbol{n}_T) \otimes (\boldsymbol{n} \otimes \boldsymbol{n}_T) \tag{13}$$

The constitutive model of the concrete matrix is based on a linear normal-tangential strength criterion. The yield condition in hardening/softening regime is defined by the unified equation

$$F(\boldsymbol{t}, \kappa) = \alpha |\boldsymbol{\sigma}_T| + \sigma_N - (f_t' - K(\kappa)) = 0 \quad , \quad \alpha = \frac{f_t'}{\tau_y'} \tag{14}$$

being f_y' and τ_y' the tensile and shear strength, respectively.

The evolution of the internal variable is defined in terms of the plastic parameter rate $\dot{\lambda}$ as

$$\dot{\kappa} = \frac{\partial F}{\partial K} = \dot{\lambda} \tag{15}$$

A non-associated flow is adopted in order to avoid the excessive inelastic dilatancy. The plastic potential Q is based on a volumetric modification of the yield condition by η, non-associativity parameter

$$Q(\boldsymbol{t}, \kappa) = |\boldsymbol{\sigma}_T| + \eta \alpha \sigma_N - (f_t' - K(\kappa)) = 0 \tag{16}$$

Then, gradient tensor $\boldsymbol{m}$ to the plastic potential can be obtained by a modification of the gradient tensor $\boldsymbol{n}_\sigma$ to the yield surface as

$$\boldsymbol{m} = \begin{bmatrix} m_{\sigma_N} \\ \boldsymbol{m}_{\sigma_T} \end{bmatrix} = \begin{bmatrix} \eta n_{\sigma_N} \\ \boldsymbol{n}_{\sigma_T} \end{bmatrix} \tag{17}$$

In post-peak regime the evolution of the dissipative stress, due to micro-fracture process at the microplane level, is defined through the homogenization process of the fracture energy released in the discontinuous with the plastic dissipation of an equivalent continuum of the same high, similarly to the fracture energy-based plasticity model by Willam et al. (1985) and Etse and Willam (1994), as

$$\dot{K} = f_t' \left[1 - exp \left(-5 \frac{h_t}{u_r} \frac{G_f^I}{G_f^{IIa}} \dot{\varepsilon}_f \right) \right] \tag{18}$$

with the equivalent fracture strain

$$\dot{\varepsilon}_f = |\boldsymbol{m}| \dot{\kappa} \tag{19}$$

where h_t represents the characteristic length associated with the active fracture process and, more specifically, the distance or separation between microcracks. Moreover, u_r represents the maximum crack opening displacement in mode I type of failure. G_f^I and G_f^{IIa} are the fracture energies in modes I and II of failure, respectively.

In the special case of uniaxial tension state, the evolution of the dissipative stress can be obtained with the simplified expression

$$\dot{K} = f_t' \left[1 - exp \left(-5 \frac{h_t}{u_r} \dot{\varepsilon}_f \right) \right] \tag{20}$$

5 FIBER-CONCRETE INTERACTION

In this section the interaction between steel fibers to cementitious matrix in form of bond-slip axial behavior and dowel action is presented.

5.1 Bond-slip model of steel fiber

The uniaxial behavior of the steel fiber is approached thought a simple 1D elasto-plastic model. The incremental stress-strain relationship, can be written as

$$\dot{\sigma_f} = E_f^{ep}\dot{\varepsilon}_N \tag{21}$$

where the elasto-plastic tangent module E_f^{ep} takes the two distinct following values

$$\begin{cases} E_f^{ep} = E_f & \rightarrow \text{Elastic response} \\ E_f^{ep} = E_f \frac{1}{E_f/H_f+1} & \rightarrow \text{Elasto-plastic regime} \end{cases} \tag{22}$$

where assuming a serial structural system constituted by the fiber response and the fiber-to-concrete joint, the corresponding total deformability $1/E_f$ is given by

$$\frac{1}{E_f} = \frac{1}{E_s} + \frac{1}{E_d} \tag{23}$$

being E_s and E_d the steel Young's module and an equivalent interface module of matrix-fiber interface, respectively. To complete the bond-slip axial constitutive models presented by the Eqs. (21) and (22), the following parameters have been considered

$$\sigma_{y,f} = min[\sigma_{y,s}, \sigma_{y,d}]$$

and

$$H^f = \begin{cases} H^s & \text{If } \sigma_{y,s} < \sigma_{y,d} \\ H^d & \text{otherwise} \end{cases}$$

being $\sigma_{y,f}$ the debonding strength value, H^f the strain-softening internal variable, $\sigma_{y,s}$ the yield limit of material and $\sigma_{y,d}$ the equivalent interface elastic limit. The supra-indexes s and d refer to steel and debonding. Further analytical details can be found in Caggiano et al. (2010).

5.2 Mechanical dowel behavior of fiber-to-concrete interaction

The dowel effect can be treated considering each fiber as a semi-infinite beam on elastic foundation (Winkler theory) in order to model the interaction between the fibers crossing the surrounding cracked medium. Considering for simplicity that the cracks develops in the middle of the fiber length, at $l_f/2$ for each one, the transferred load-action between fiber and concrete by means a dowel effect can be analyzed as a concentrated load representing the dowel resultant V_d

$$V_d = E_s I_s \lambda^3 \Delta \tag{24}$$

where $I_s = \pi d_f^4/64$ is the moment of inertia of the fiber (d_f diameter of the fiber), Δ represents the dowel displacement and the parameter λ the relative stiffness between the fiber and the foundation, which is given by

$$\lambda = \sqrt[4]{\frac{k_c d_f}{4E_s I_s}} \tag{25}$$

where k_c is the foundation module of the surrounding matrix which typical values, for standard RC structures, ranges from 75 to 450 N/mm^3 (Dei Poli et al., 1992). An equivalent shear elastic module can be calculated as follows

$$V_d = E_s I_s \lambda^3 \Delta = \frac{\Delta}{L_f} A_f \Rightarrow G_f = E_s I_s \lambda^3 \frac{L_f}{A_f} \tag{26}$$

where $A_s = \pi d_f^2/4$ is the cross area section of the bar.

Finally the following equation, proposed by Dulacska (1972) for estimating the dowel action at ultimate limit state V_{du} is used

$$V_{du} = k_{dow} d_f^2 \sqrt{|f_c'||\sigma_{y,s}|} \tag{27}$$

being k_{dow} is a non-dimensional coefficient (k_{dow} =1.27, for RC-structures), while f_c' is the compressive strength of the surrounding cement-based material.

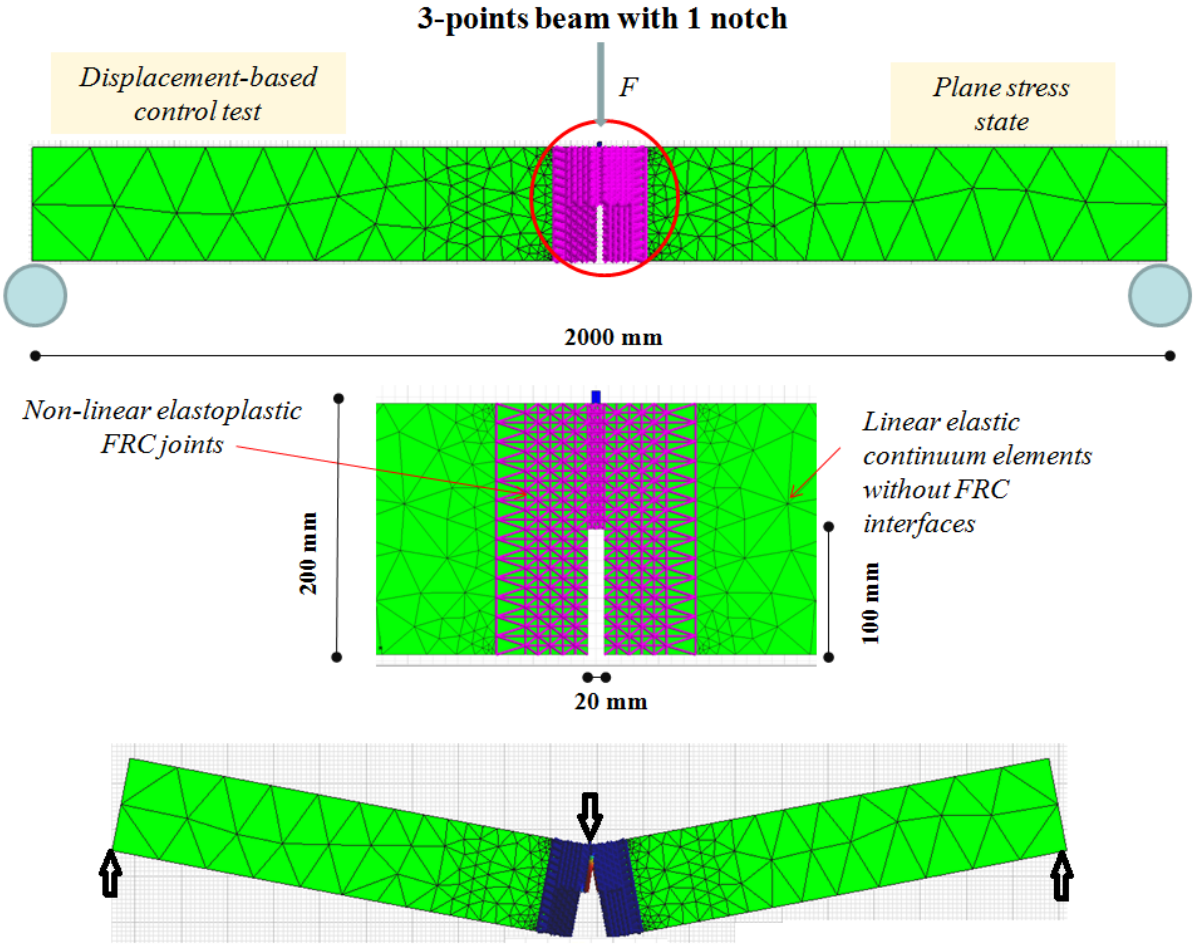

Figure 4: three point bending test on a notched beam

6 NUMERICAL ANALYSIS

In this section several numerical analysis are performed by means both the mesoscopic and macroscopic models regarding failure behavior at structural (on FRC structural members) and material level, respectively.

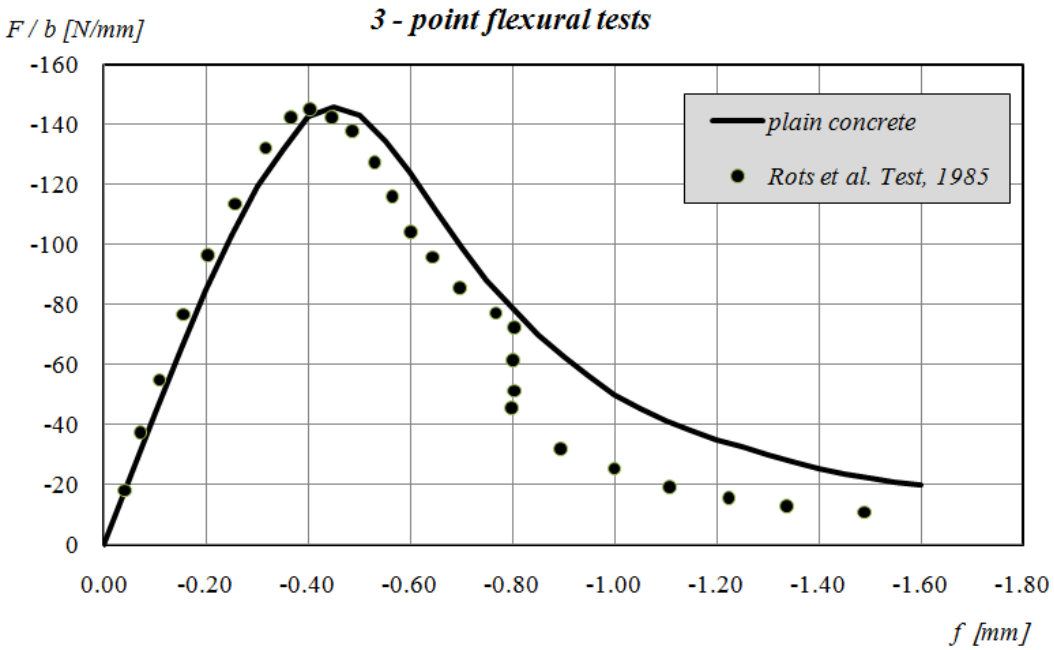

Figure 5: Numerical vs. experimental comparison on 3-p flexural tests on plain concrete beam

6.1 Mesoscopic failure analysis on 3-point flexural notched beams

To evaluate the predictive capabilities of the proposed non-linear cracking model for FRC the 3-point flexural scheme shown in Fig. 4 is considered. Several interface elements have been placed between two bidimensional and isoparametric three node elements in order to model the fracture process of the beam loaded in a "3-point" manner as indicated in Fig. 4.

Five different steel fiber volume contents are considered, i.e. $\rho_f = 0,\ 1,\ 2,\ 3$ and 6%, all with the same diameter $d_f = 0.8\,mm$. Plane stress conditions (considering a depth of the beam $b = 50\,mm$) is imposed in the numerical analysis at the mesoscopic level of observation.

Firstly, a plain concrete test is performed by imposing homogeneous vertical displacement at mid-length of the considered beam. The results in terms of vertical applied deflection f vs. vertical measured unitary force F/b are shown in Fig. 5 when the test is compared against the experimental measures performed by Rots et al. (1985).

Furthermore the results in Fig. 6, performed with different amount of fibers ($d_f = constant = 0.8\,mm$) indicate that the proposed model is able to reproduce the sensitivity of FRC in terms of post-peak ductility. The post-peak responses is characterized by a reloading effect typical in FRC, dealing with the activation of the fiber only in cracked regime.

The Fig. 6 emphasizes a clear phenomenological behavior of FRC, depending on the fiber content. A progressive transition of the stress-strain relationship form the typical softening behavior of plain concrete toward a more ductile behavior can be observed for the various values of fiber content, ranging from 1% to 6% in the analyzed cases. In conclusion, the proposed interface model for mesoscopic analysis of FRC failure behavior shows realistic predictions of peak stresses, ductility and post-peak behavior of this material when different fiber contents are considered.

Table 1 outlines the values of the key parameters related to the analysis of the 3-point flexural tests.

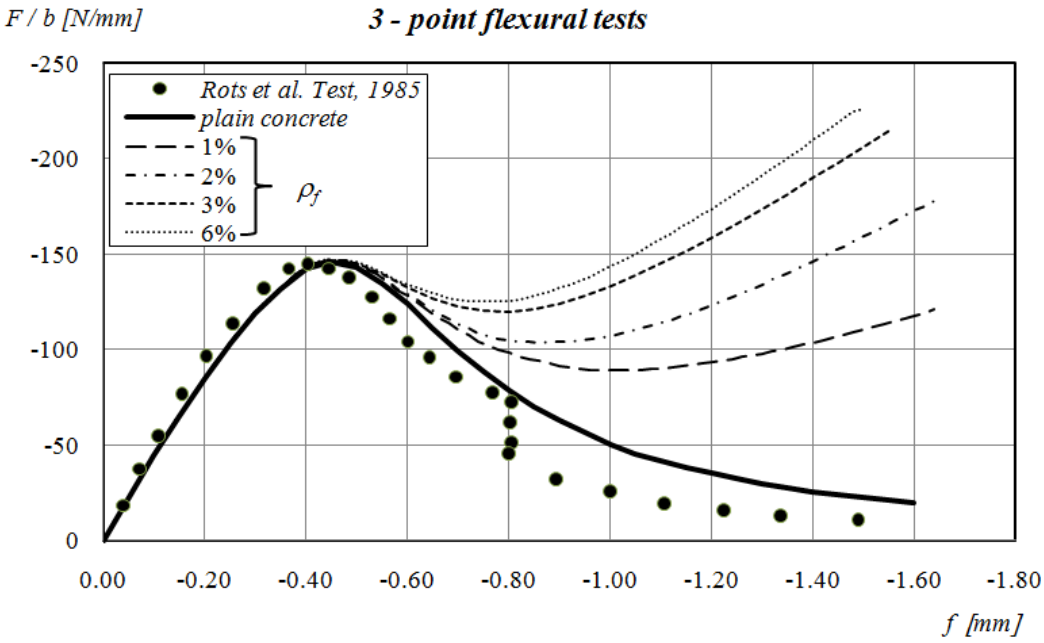

Figure 6: Force - displacement relationship on 3-p flexural tests with different of fiber contents

Continuum elements						
		E_m [MPa]			ν	
		30000			0.2	
Interface Elements						
K_N [MPa/mm]	K_T [MPa/mm]	χ [MPa]	c [MPa]	tg ϕ	G_f^I [N/mm]	G_f^{II} [N/mm]
1.E+06	1.E+06	3.33	5	0.5	0.124	1.240
Steel Fibers						
bond-slip			*dowel*			
E_f [GPa]	σ_{yf} [MPa]	H_f [GPa]		k_c [MPa]	f'_c [MPa]	
35	258	0		257	33.3	

Table 1: Material parameters of the 3-point concrete beam

6.2 Macroscopic FRC failure analysis

In this section the preliminary numerical studies to evaluate the capabilities to simulate failure behavior of FRC of the proposed macroscopic model, based on microplane theory, are performed. Unidirectional and an isotropic fiber distribution are considered with different fiber volume contents (i.e. $\rho_f = 0.3$ and 0.6%) also including the extreme case of plain concrete ($\rho_f = 0$). The steel fiber material parameters are shown in Table 1, while the material parameters corresponding to the concrete matrix are $E = 19000\,MPa$, $\nu = 0.2$, $f'_c = 22\,MPa$, $f'_t = 3.0\,MPa$, $h_t = 108\,mm$, $u_r = 0.127\,mm$, $G_f^{IIa}/G_f^I = 10$.

Considering a single element problem in plane strain conditions subjected to an homogeneous stress/strain state: therein uniaxial tension, uniaxial compression and shear tests are performed.

Firstly, the results of uniaxial tensile test with fibers oriented in the loading direction and with isotropic distribution are illustrated in Fig. 7. The elastic stiffness increases in case of bias

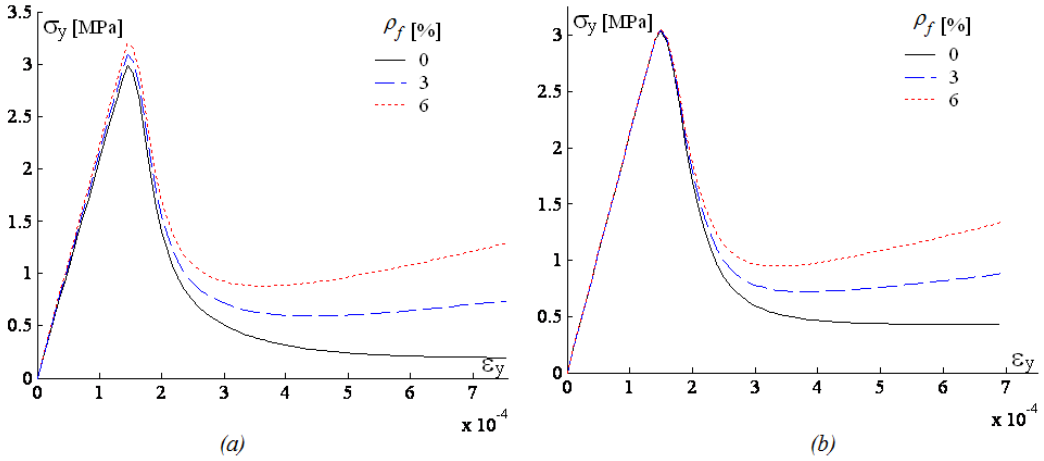

Figure 7: Uniaxial tensile test for microplane model: a) Fibers oriented in loading direction; b) Isotropic fiber distribution.

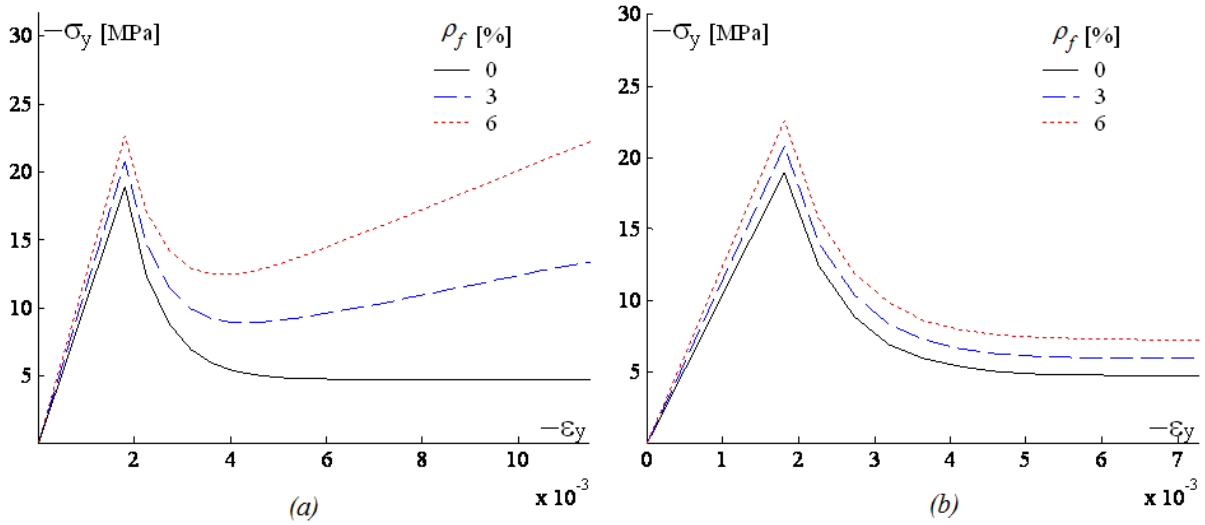

Figure 8: Uniaxial compression test for microplane plasticity: a) Fibers oriented in loading direction; b) Isotropic fiber distribution.

fiber as compared to the plain concrete case and with the increment of ρ_f.

The results obtained in the uniaxial compression test with both uniaxially oriented fibers and an isotropic distribution of fiber directions are shown in Fig. 8. In case of bias fiber, as expected, the stiffness in the pre-peak regime and the overall dissipated energy during post-peak regime increase with ρ_f.

Finally, the shear tests results depict in Fig. 9 demonstrate in the both cases, bias and isotropic fiber distribution, that the stiffness increases in the pre-peak regime and the ductility in pre and post-peak regimes.

7 CONCLUSIONS

Mesoscopic and macroscopic models for fiber reinforced cement composite materials have been presented. The mesoscopic model takes into account a three phase mesostructure composed by elastic aggregates, mortar and mortar-aggregate interfaces. This model also includes

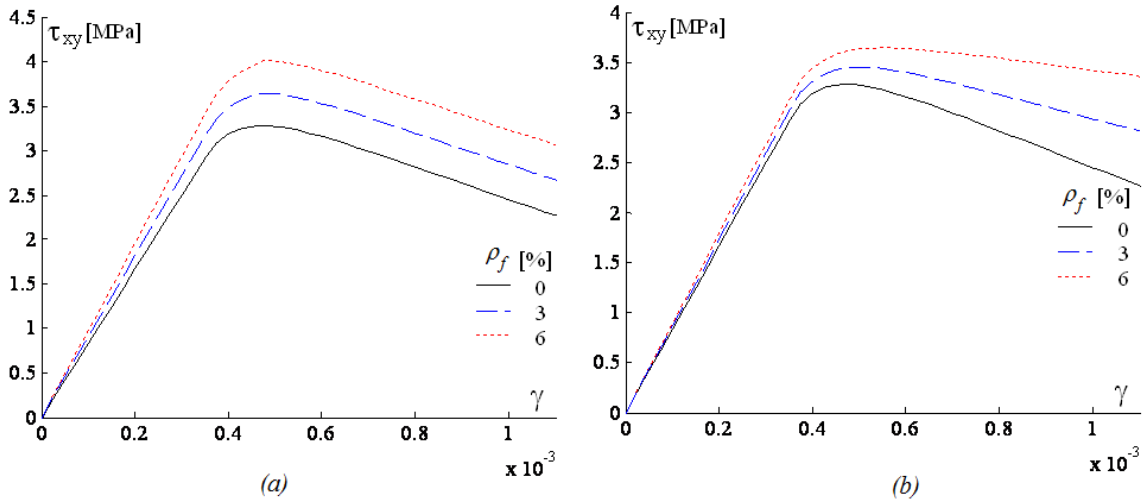

Figure 9: Shear test for microplane plasticity: a) Fibers oriented in loading direction; b) Isotropic fiber distribution.

mortar-mortar interfaces to simulate the dissipative response behavior of this constituent. Macroscopic model is formulated within the theoretical framework of microplane theory. Both the interface model and the microplane model for meso- and macroscopic analyses, respectively, are based on flow rule of plasticity, mixing theory by Truesdell and Toupin (1960) and composite model by Oliver et al. (2008). Thereby, the interaction between steel fibers and mortar/concrete accounts for debonding and dowel effects. Numerical analyses with both constitutive models in this paper demonstrate their capabilities to reproduce the most relevant aspects of failure behavior of steel fiber reinforced concretes under tensile, shear and compressive stresses.

8 ACKNOWLEDGEMENTS

The first and third authors acknowledge the financial support for this work by FONCYT (Argentine agency for the promotion of research and technology) through the Grant PICT No. 1232/6, by CONICET (Argentine National Council for Science and Technology) through the Grant PIP No. 6201/05 and by CIUNT (Research Council University of Tucuman) through the Grant No. E/26 455. The second author acknowledges to the financial support provided by the University of Salerno and by MIUR (Italian Ministry for Education, University and Research).

REFERENCES

Banholzer B., Brameshuber W., and Jung W. Analytical evaluation of pull-out tests-the inverse problem. *Cement & Concrete Composites*, 28:564–571, 2006.

Beghini A., Bazant Z., Zhou Y., Gouirand O., and Caner F. Microplane model m5f for multiaxial behavior and fracture of fiber-reinforced concrete. *ASCE - Journal of Engineering Mechanics*, 133:66–75, 2007.

Caggiano A., Etse G., and Martinelli E. Fracture-energy-based interface theory for fiber reinforced concrete failure analyses. *The new boundaries of structural concrete, Proceedings of ACI Italy Chapter, Fisciano/Salerno, Italy, April*, 2010.

Carol I., Jirásek M., and Bazănt Z. A thermodynamically consistent approach to microplane theory. part i. free energy and consistent microplane stresses. *Int. Journal of Solids and Structures*, 38:2933–2952, 2001.

Carol I., Prat P., and Lopez C. Normal/shear cracking model: Applications to discrete crack

analysis. *ASCE - Journal of Engineering Mechanics*, 123:765–773, 1997.

Carpinteri A., Chiaia B., and Invernizzi S. Three-dimensional fractal analysis of concrete fracture at the meso-level. *Theoretical and Applied Fracture Mechanics*, 31:163–172, 2010.

Cusatis G., Schauffert E., Pelessone D., O'Daniel J., Marangi P., Stacchini M., and Savoia M. Lattice discrete particle model for fiber reinforced concrete (ldpm-f) with application to the numerical simulation of armoring systems. *EURO-C 2010, Computational Modeling of Concrete Structures*, 1:291–300, 2010.

Dei Poli S., Di Prisco M., and Gambarova P. Shear response, deformations, and subgrade stiffness of a dowel bar embedded in concrete. *ACI - Structural Journal*, 89:665–675, 1992.

Dulacska H. Dowel action of reinforcement crossing cracks in concrete. *ACI - Structural Journal*, 69:754–757, 1972.

Etse G. and Willam K. A fracture energy-based constitutive theory for inelastic behavior of plain concrete. *ASCE - Journal of Engineering Mechanics*, 120:1983–2011, 1994.

Hu X., Day R., and Dux P. Biaxial failure model for fiber reinforced concrete. *ASCE - Journal of Material in Civil Engineering*, 15:609–615, 2003.

Kuhl E., Steinmann P., and Carol I. A thermodynamically consistent approach to microplane theory. part ii. disipation and inelastic constitutive modeling. *Int. Journal of Solids and Structures*, 38:2921–2931, 2001.

Li F. and Li Z. Continuum damage mechanics based modeling of fiber reinforced concrete in tension. *Int. Journal of Solids and Structures*, 38:777–793, 2001.

Lilliu G. and van Mier J. 3d lattice type fracture model for concrete. *Engineering Fracture Mechanics*, 70:927–941, 2003.

Lopez C.M., Carol I., and Aguado A. Meso-structural study of concrete fracture using interface elements. i: numerical model and tensile behavior. *Materials and Structures*, 41:583–599, 2008a.

Lopez C.M., Carol I., and Aguado A. Meso-structural study of concrete fracture using interface elements. ii: compression, biaxial and brazilian test. *Materials and Structures*, 41:601–620, 2008b.

Lorefice R., Etse G., and Carol I. Viscoplastic approach for rate-dependent failure analysis of concrete joints and interfaces. *Int. Journal of Solids and Structures*, 45:2686–2705, 2008.

Naaman A.E. and Reinhardt H.W. Proposed classification of frc composites based on their tensile response. *Materials and Structures*, 39:547–555, 2006.

Oliver J., Linero D., Huespe A., and Manzoli O. Two-dimensional modeling of material failure in reinforced concrete by means of a continuum strong discontinuity approach. *Comput. Methods Appl. Mech. Engrg.*, 197:332–348, 2008.

Park H. and Kim H. Microplane model for reinforced-concrete planar members in tension-compression. *Journal of Structural Engineering*, 129:337–345, 2003.

Pietruszczak S. and Winnicki A. Constitutive model for concrete with embedded sets of reinforcement. *ASCE - Journal of Engineering Mechanics*, 129:725–738, 2003.

Rots J., Nauta P., Kusters G., and Blaauwendraad J. *Smeared Crack Approach And Fracture Localization In Concrete*, volume 30. McGraw Hill, 1985.

Seow P.E.C. and Swaddiwudhipong S. Failure surface for concrete under multiaxial load - a unified approach. *ASCE - Journal of Material in Civil Engineering*, 17:219–228, 2005.

Truesdell C. and Toupin R. *Classical Field Theories of Mechanics*, volume III/1. Handbuch der Physik, Springer Verlag, 1960.

Vrech S., Etse G., Meschke G., Caggiano A., and Martinelli E. Meso and macroscopic models for fiber-reinforced concrete. *EURO-C 2010, Computational Modeling of Concrete Struc-*

tures, 1:241–250, 2010.

Willam K., Hurbult B., and Sture S. Experimental and constitutive aspects of concrete failure. *In US-Japan Seminar on Finite Element Analysis of Reinforced Concrete Structures. ASCE-Special Publication*, 1:226–254, 1985.

Zubelewicz A. and Bazant Z. Interface element modeling of fracture in aggregate composites. *ASCE - Journal of Engineering Mechanics*, 113:1619–1630, 1987.